

Perspectives of the GAMMA-400 space observatory for high-energy gamma rays and cosmic rays measurements

N P Topchiev^{2,*}, A M Galper^{1,2}, V Bonvicini⁷, O Adriani⁸, R L Aptekar³, I V Arkhangel'skaja¹, A I Arkhangel'skiy¹, A V Bakaldin¹, L Bergstrom⁹, E Berti⁸, G Bigongiari¹⁰, S G Bobkov⁶, M Boezio⁷, E A Bogomolov³, S Bonechi¹⁰, M Bongi⁸, S Bottai⁸, G Castellini¹¹, P W Cattaneo¹², P Cumani⁷, O D Dalkarov², G L Dedenko¹, C De Donato¹³, V A Dogiel², N Finetti⁸, M S Gorbunov⁶, Yu V Gusakov², B I Hnatyk¹⁴, V V Kadilin¹, V A Kaplin¹, A A Kaplun¹, M D Kheymits¹, V E Korepanov¹⁵, J Larsson¹⁶, A A Leonov^{1,2}, V A Loginov¹, F Longo⁷, P Maestro¹⁰, P S Marrocchesi¹⁰, A L Men'shenin⁴, V V Mikhailov¹, E Mocchiutti⁷, A A Moiseev¹⁷, N Mori⁸, I V Moskalenko¹⁸, P Yu Naumov¹, P Papini⁸, M Pearce¹⁶, P Picozza¹³, A Rappoldi¹², S Ricciarini¹¹, M F Runtso¹, F Ryde¹⁶, O V Serdin⁶, R Sparvoli¹³, P Spillantini⁸, Yu I Stozhkov², S I Suchkov², A A Taraskin¹, M Tavani¹⁹, A Tiberio⁸, E M Tyurin¹, M V Ulanov³, A Vacchi⁷, E Vannuccini⁸, G I Vasilyev³, Yu T Yurkin¹, N Zampa⁷, V N Zirakashvili⁵ and V G Zverev¹

¹ National Research Nuclear University MEPhI (Moscow Engineering Physics Institute), Kashirskoe highway 31, Moscow, 115409, Russia

² Lebedev Physical Institute, Russian Academy of Sciences, Moscow, Russia

³ Ioffe Institute, Russian Academy of Sciences, St. Petersburg, Russia

⁴ Research Institute for Electromechanics, Istra, Moscow region Istra, Russia

⁵ Pushkov Institute of Terrestrial Magnetism, Ionosphere, and Radiowave Propagation, Troitsk, Moscow region, Russia

⁶ Scientific Research Institute for System Analysis, Russian Academy of Sciences, Moscow, Russia

⁷ Istituto Nazionale di Fisica Nucleare, Sezione di Trieste and Physics Department of University of Trieste, Italy

⁸ Istituto Nazionale di Fisica Nucleare, Sezione di Firenze and Physics Department of University of Florence, Firenze, Italy

⁹ Stockholm University, Department of Physics; and the Oskar Klein Centre, AlbaNova University Center, Stockholm, Sweden

¹⁰ Department of Physical Sciences, Earth and Environment, University of Siena and Istituto Nazionale di Fisica Nucleare, Siena, Italy

¹¹ Istituto di Fisica Applicata Nello Carrara - CNR and Istituto Nazionale di Fisica Nucleare, Sezione di Firenze, Firenze, Italy

¹² Istituto Nazionale di Fisica Nucleare, Sezione di Pavia, Pavia, Italy

¹³ Istituto Nazionale di Fisica Nucleare, Sezione di Roma 2 and Physics Department of University of Rome Tor Vergata, Rome, Italy

¹⁴ Taras Shevchenko National University of Kyiv, Kyiv, Ukraine

¹⁵ Lviv Center of Institute of Space Research, Lviv, Ukraine

¹⁶ KTH Royal Institute of Technology, Department of Physics, and the Oskar Klein Centre, AlbaNova University Center, Stockholm, Sweden



¹⁷ CRESST/GSFC and University of Maryland, College Park, Maryland, USA

¹⁸ Hansen Experimental Physics Laboratory and Kavli Institute for Particle Astrophysics and Cosmology, Stanford University, Stanford, USA

¹⁹ Istituto Nazionale di Astrofisica IASF and Physics Department of University of Rome Tor Vergata, Bologna, Italy

*leon@ibrae.ac.ru

Abstract. The GAMMA-400 gamma-ray telescope is intended to measure the fluxes of gamma-rays and cosmic-ray electrons and positrons in the energy range from 100 MeV to several TeV. Such measurements concern the following scientific tasks: investigation of point sources of gamma-rays, studies of the energy spectra of Galactic and extragalactic diffuse emission, studies of gamma-ray bursts and gamma-ray emission from the Sun, as well as high precision measurements of spectra of high-energy electrons and positrons. Also the GAMMA-400 instrument provides the possibility for protons and nuclei measurements up to knee. But the main goal for the GAMMA-400 mission is to perform a sensitive search for signatures of dark matter particles in high-energy gamma-ray emission. To fulfill these measurements the GAMMA-400 gamma-ray telescope possesses unique physical characteristics in comparison with previous and present experiments. The major advantage of the GAMMA-400 instrument is excellent angular and energy resolution for gamma-rays above 10 GeV. The GAMMA-400 experiment will be installed onboard of the Navigator space platform, manufactured by the NPO Lavochkin Association. The expected orbit will be a highly elliptical orbit (with apogee 300.000 km and perigee 500 km) with 7 days orbital period. An important profit of such an orbit is the fact that the full sky coverage will always be available for gamma ray astronomy.

1. Introduction

The GAMMA-400 observatory will allow to address a broad range of science topics, like search for signatures of dark matter, studies of Galactic and extragalactic gamma-ray sources, Galactic and extragalactic diffuse emission, gamma-ray bursts and charged cosmic rays acceleration and diffusion mechanism up to the knee. GAMMA-400 will be able to study gamma-rays, from 100 MeV up to several TeV, electrons up to 10 TeV, protons and nuclei up to the knee (10^{15} – 10^{16} eV). It will search for possible dark matter signal thanks to an unprecedented energy resolution that will permit to detect features associated with dark matter annihilation or decay in the spectra of Galactic Center region [1].

The GAMMA-400 will be installed onboard the Russian Space Observatory.

2. The GAMMA-400 gamma-ray telescope

The GAMMA-400 physical scheme is shown in figure 1. Starting from the top, the telescope is composed by the following layers:

- an anticoincidence system (AC) is composed by plastic scintillators, located both on top and on the lateral side of the apparatus. AC is essentially used to veto charged particles.
- a converter-tracker system (C) consists of 13 layers of double (x, y) silicon strip coordinate detectors (pitch 0.08 mm). The first three and final two layers have no tungsten while the middle eight layers are interleaved with tungsten conversion foils. The thickness of tungsten is $0.1 X_0$. The total converter-tracker thickness is about $1 X_0$. Using the first three layers without tungsten allows to measure gamma rays from approximately 20 MeV. The system is used to convert the photons and precisely reconstruct the photon direction by the detection in the silicon layers the conversion e^+e^- pair.
- a Time of Flight system (ToF) is formed by plastic scintillators S1 and S2, separated by approximately 500 mm. This system is used both to generate the trigger for the apparatus and to reject albedo particles by measuring their velocity.

- an imaging calorimeter CC1. CC1 is composed by 2 layers of CsI(Tl) crystals, each $1 X_0$ deep, interleaved with 2 silicon microstrip layers of the same type used for the converter-tracker. The thickness of CC1 is $2X_0$. The imaging calorimeter is used to significantly improve the photon angular resolution by precisely measuring the conversion e^+/e^- pair after a large 50 cm lever arm below the converter-tracker.
- the scintillation detectors S3 and S4 improve hadrons/electron separation.
- deep, isotropic and homogeneous electromagnetic calorimeter (CC2) is composed by $28 \times 28 \times 12$ small cubic CsI(Tl) crystals (with 3.6 cm side), developed on the basis of the CaloCube project R&D [4]. The overall dimensions of the calorimeter are the following: $1 \text{ m} \times 1 \text{ m} \times 0.48 \text{ m}$, corresponding to $54.6 X_0 \times 54.6 X_0 \times 23.4 X_0$ and $2.5 \lambda_1 \times 2.5 \lambda_1 \times 1.1 \lambda_1$. Using a deep calorimeter allows us to extend the energy range up to several TeV for gamma rays and to reach an energy resolution of approximately 1% above 100 GeV. The overall mass ($\sim 2000 \text{ kg}$), coupled to the large dimensions, will allow detection of high energy hadrons, up to 10^{15} eV , with an effective geometric factor of the order of $4 \text{ m}^2 \times \text{sr}$, giving the possibility to directly probe on orbit the knee region. This is accomplished by detecting particles not only on the top surface, but also on the lateral side, hence significantly increasing the overall geometrical factor.
- a neutron detector (ND), located below the CC2, is used to improve the proton/electron separation.

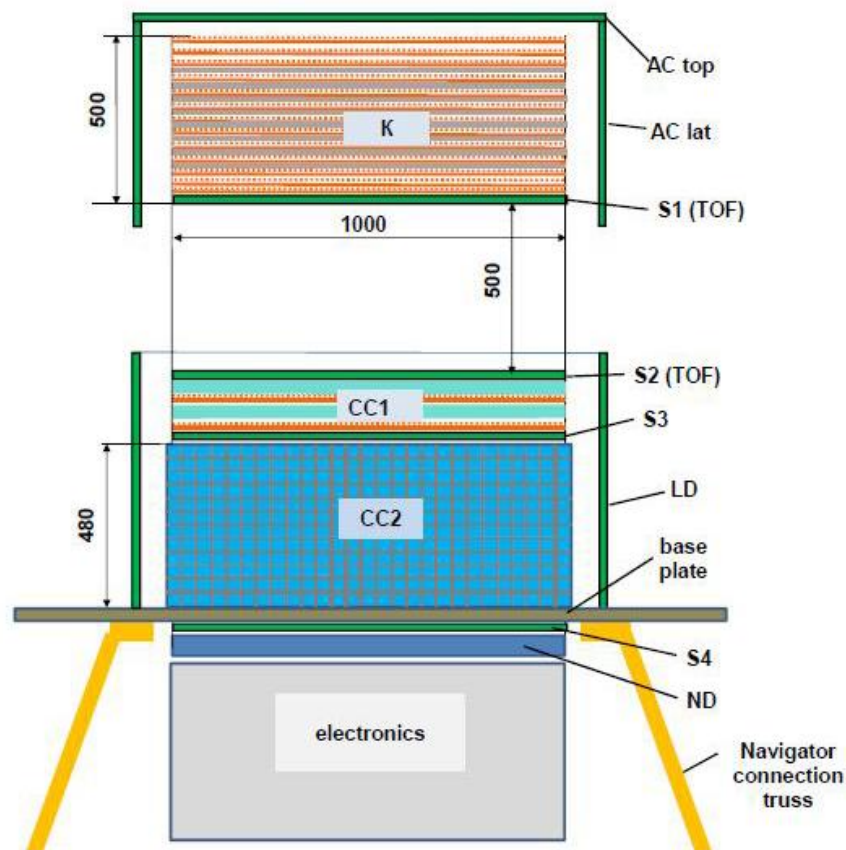


Figure 1. Schematic drawing of the GAMMA-400 telescope.

3. The GAMMA-400 gamma-ray telescope performance

To calculate GAMMA-400 instrument performance the following main trigger for gamma registration was used: the signal from energy release in S1 has to be before than the signal in S2 and the signal in

AC system has to be less than the value of threshold selected in such way to suppress the back splash influence. For what concern the instrument's performances in the gamma detection. Figures 2 and 3 show respectively the effective area, the angular and the energy resolution of the GAMMA-400 telescope.

In figure 2a the dependence of effective area from initial energy of vertical gamma rays and in figure 2b the dependence of effective area from the incidence angle of the initial 100-GeV gamma are presented. These curves were obtained taking into account the main trigger signal of GAMMA-400: S1 & S2 & (no AC). Time and segmentation methods are used to reduce the influence of backscattering particles created when incident γ -rays interact with the calorimeter's matter and produce low energy photons, electrons... moving in the opposite direction [5]. The effective area of GAMMA-400 is approximately twice lower than total effective area of Fermi-LAT [6,7]. However, for a full comparison of the performances it is necessary to take into account the optimized choice of the pointing strategy for important sources or for the whole sky survey, considering that the full sky is available to GAMMA-400, due to the peculiar orbit, very far away from any possible earth occultation. Moreover, the high energy part of the photon spectrum can be investigated with the calorimeter CC2 only, with an angular resolution better than two degrees. This way the acceptance can be significantly increased, reaching a level of $\sim 4 \text{ m}^2$.

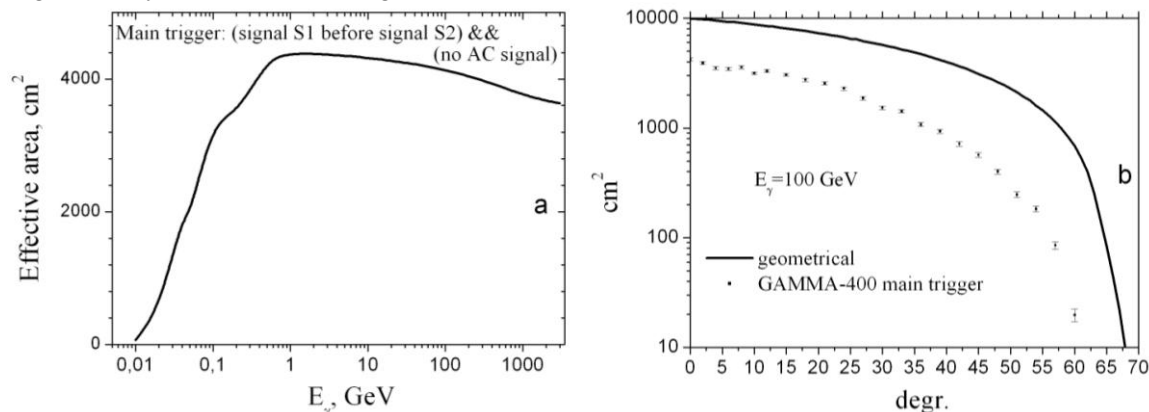


Figure 2. Effective area of GAMMA-400 in the photon detection. a) The dependence of effective area from initial energy of gamma with vertical incidence. b) The dependence of effective area from the incidence angle of the initial 100 GeV gamma.

The angular resolution of GAMMA-400 is comparable to the Fermi-LAT in the 100 MeV - few GeV range, while it is significantly better above few GeV (figure 3a). This is accomplished by a proper combination of the excellent spatial resolution and the long lever arm available in between the converter-tracker and the CC1 calorimeter. The low energy part (less than 500 MeV) of GAMMA-400 angular resolution curve was obtained for gamma events converted in the upper thin layers of converter-tracker system. Taking into account the power-law behaviour of gamma spectrum, the reducing of effective area is not so important for such energies.

The performance of the instrument for what concern the energy resolution is demonstrated in figure 3b. It is clearly better than Fermi-LAT one above few hundreds MeV, reaching a resolution better than 2% for the multi GeV range. This is possible thanks to the excellent performances of the homogeneous and deep calorimeter, able to fully absorb electromagnetic shower generated by multi-GeV photons.

The characteristics of GAMMA-400 instrument will allow exploring high energy gamma from any space region in more details in comparison with FERMI-LAT. To demonstrate the advantage of GAMMA-400 capabilities the center of Galaxy region ($-1 < l < 0.76$; $0.285 < b < 0.3$) was selected concerning possible location of Dark Matter particles [8, 9]. In this region there are four point sources identified in third source FERMI-LAT catalog [10]. Using information about the energy spectrum and total intensity for these sources in the energy range 10-100 GeV, and diffuse flux from background

models [11] it is possible to simulate the energy distribution for gamma events identified in the vicinity of Galactic center during FERMI-LAT mission. This distribution is shown in figure 4 (green color). The value of energy bin for this distribution was selected equal 10 GeV according to the value 0.1 of FERMI-LAT relative energy resolution about 100 GeV. If there is some energetic gamma line with energy 85 GeV, providing 25 gamma events for FERMI-LAT effective area during total time of the mission, then energy distribution will change (blue color in figure 4a). The magnified view of sum energy distribution is shown in figure 4b. It is evidently that it is impossible to identify some additional source with enough statistic significance having such energy resolution. But if the energy distribution would be build with energy bin 2 GeV according to energy resolution of GAMMA-400, than additional source could be easy identified. In figure 5a the energy distributions for the ordinary gamma (red color) and for the gamma from line (blue color) with the value of bin 2 GeV are shown. In figure 5b the magnified view of sum energy distribution is shown. In four bins with additional gamma from line 85 GeV there are 25 events from the additional source and 7 events from the ordinary gamma. So, the level of significance 4 sigma is provided and the additional flux of gamma $\sim 10^{-10} \text{ cm}^{-2} \text{ sec}^{-1}$ can be identified.

FERMI (http://www.slac.stanford.edu/exp/glast/groups/canda/lat_Performance.htm)

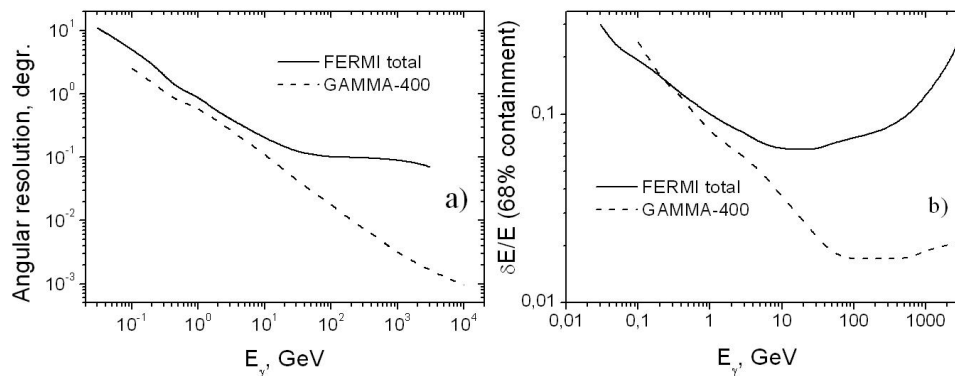


Figure 3. The angular and energy resolutions of GAMMA-400 in the photon detection. a) The dependence of angular resolution from initial energy of gamma. b) The dependence of energy resolution from initial energy of gamma. The characteristics of FERMI-LAT are also presented.

The GAMMA-400 observatory is also an optimal tool for the very high energy hadron detection. For this item two critical parameters exist in the detection system: the acceptance, that should be as large as possible, to have the possibility to measure a significant amount of the 10^{15} eV particles, and the hadronic energy resolution. The large area homogeneous and isotropic calorimeter, accepting particles from all sides, gives us for the first time the possibility to directly observe in space such high energy hadrons. Figure 6 shows the expected number of high energy protons and helium nuclei for a 10 years exposure of the GAMMA-400 experiment, assuming the Polygonato model [12], with an expected p/e rejection factor better than 10^5 [3], and with a realistic reconstruction efficiency of the order of 40%. It is expected to collect a statistic larger than 100 events with energy $\sim 10^{15}$ eV both for protons and helium, allowing a detailed probe of the interesting knee region, that has never been directly investigated with an in orbit detector up to now.

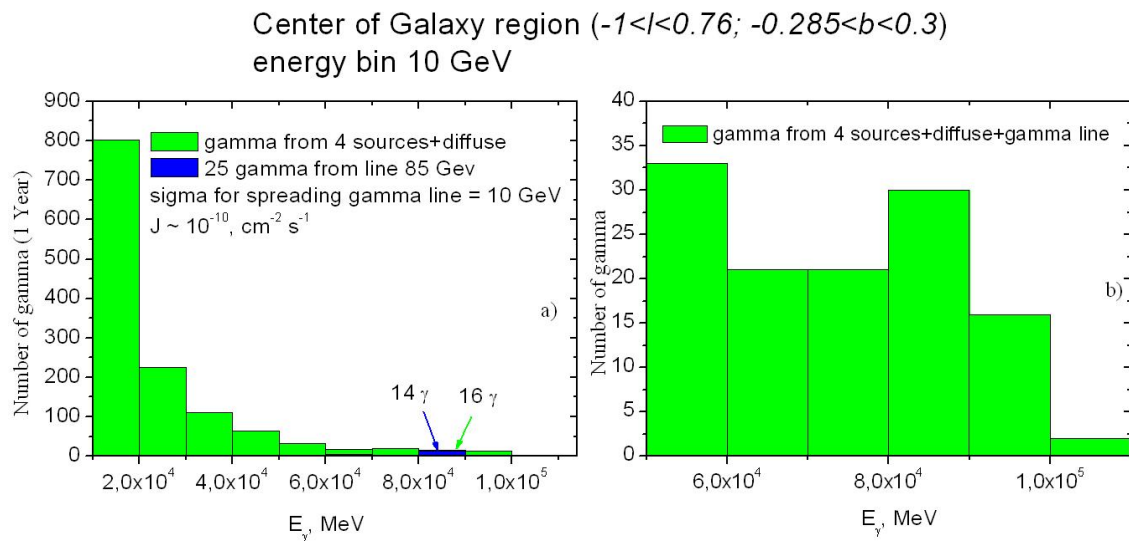


Figure 4. a) The energy distribution with the value of bin equal 10 GeV for the experimental data obtained during FERMI-LAT mission in the vicinity of Galactic center for energy range 10-100 GeV and selected for maximum zenith angle less, than 90° (green color) and additional contribution from line 85 GeV (blue color) b) The magnified view of the sum energy distribution.

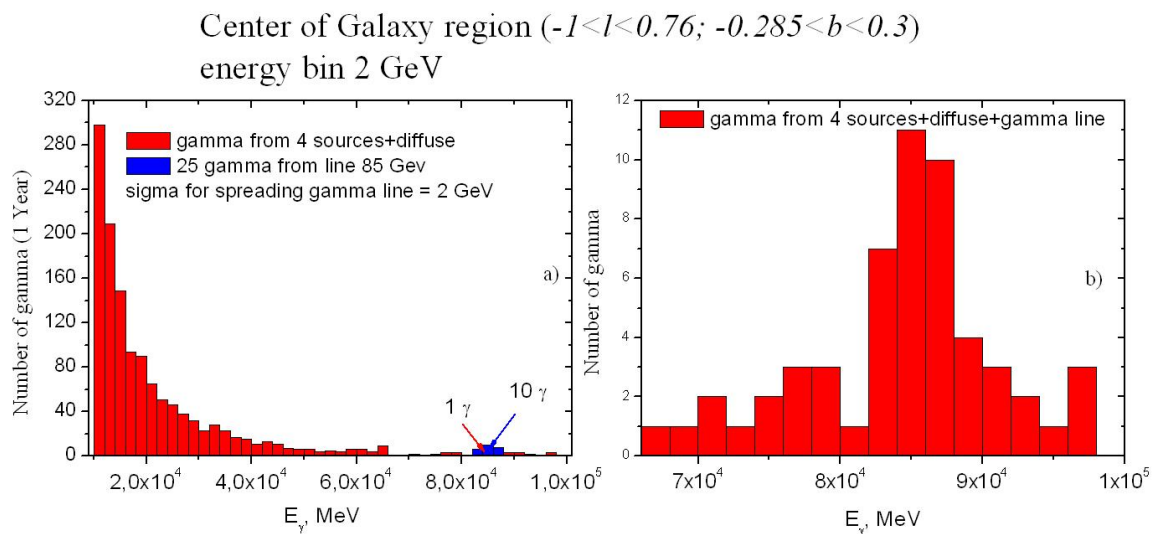


Figure 5. a) The energy distribution with the value of bin equal 2 GeV for the experimental data as in figure 4a (red color) and additional contribution from line 85 GeV (blue color). b) The magnified view of the sum energy distribution.

Protons and Helium (Polygonato model)											
Effective GF ($\text{m}^2 \text{sr}$)	$\sigma(E)/E$	$E > 0.1 \text{ PeV}$		$E > 0.5 \text{ PeV}$		$E > 1 \text{ PeV}$		$E > 2 \text{ PeV}$		$E > 4 \text{ PeV}$	
		p	He	p	He	p	He	p	He	p	He
~ 4	35%	7.8×10^3	7.4×10^3	4.6×10^2	5.1×10^2	1.2×10^2	1.5×10^2	28	43	5	10

Figure 6. Expected number of proton and helium events in 10 years data taking, according to the Polygonato model.

4. Conclusion

The GAMMA-400 instrument has been designed for the optimal detection of gamma rays in a broad energy range (from 100 MeV up to several TeV), with excellent angular and energy resolutions. The observatory will also allow precise and high statistic studies of the electron component in the cosmic rays up to the multi TeV region, as well as protons and nuclei spectra up to the knee region.

References

- [1] Galper A M *et al.* 2013 *Bull. RAS. Physics* **77**(11) 1339
- [2] Galper A M *et al.* 2013 *Adv. Space Res.* **51** 297
- [3] Leonov A A *et al.* 2015 *Adv. Space Res.* **56** 1538
- [4] Adriani O *et al.* 2013 *Proceedings of the International Conference on Calorimetry for the High Energy Frontier (CHEF)*
- [5] Ginzburg V L *et al.* 2009 *Bull. RAS. Physics* **73**(5) 664
- [6] Atwood W B *et al.* 2009 *Astropart J.* **697** 1071
- [7] Abdo A A *et al.* 2009 *Astropart Phys.* **32** 193
- [8] Hooper D & Goodenough L 2011 *Physics Letters B* **697** 412
- [9] Kaplinghat M *et al.* 20115 *Phys. Rev. Lett.* **114** 21
- [10] *FERMI-LAT catalog* (http://fermi.gsfc.nasa.gov/ssc/data/access/lat/4yr_catalog/)
- [11] URL: <http://fermi.gsfc.nasa.gov/ssc/data/access/lat/BackgroundModels.html>
- [12] Horandel J 2004 *Astropart Phys.* **21** 241